

Evaluation of Surfaces for Automobile Body Styling

Injin Choi

Computer Aided Design & Analysis Laboratory,
Dept. of Mechanical Design and Production
Engineering,
Seoul National University, Seoul, Korea
choi@CADAL1.SNU.AC.KR

Kunwoo Lee

Computer Aided Design & Analysis Laboratory,
Dept. of Mechanical Design and Production
Engineering,
Seoul National University, Seoul, Korea
kunwoo@CADAL1.SNU.AC.KR

Abstract

In the process of car body design, various surfaces can be generated from the given boundary curves. Depending upon the method of the surface generation and the quality of the boundary curves provided, the resulting surfaces may have global or local irregularities in many cases. Thus it would be necessary for the designer to evaluate the surface quality and to modify the surface or to use the different generation method based upon the evaluation results. This capability is very important because the defect of the surface quality detected in the production stage will require the rework on the dies and will cause a big loss in money and time. In this paper, two types of interrogation methods for the assessment of shape quality are described. One is the reflection mapping, which simulates the reflection test on the real part in the production line. This method is useful for detecting global irregularities of a surface. The other is the visualization of the curvature behavior of a surface. The method consists of traditional focal analysis, which exaggerates the mean, Gaussian and strain energy of curvature. This method makes it easier to detect local irregularities.

1. Introduction

One of the basic tasks in the process of automobile body styling is the design of smoothly curved forms using free-form curves and surfaces. In the course of designing free form curves and surfaces, we want the curve or surface to be "visually pleasing", in some functional or aesthetic aspect. For example, the roof of a car should not have undesirable bumps or wiggles but should be convex, and the tail of an aircraft should not have any undulations on the surface which may affect its aerodynamic properties. These kinds of undesired features of curves and surfaces result from corresponding

intrinsic geometric properties such as their curvatures and torsions. Evaluating them is referred as curve and surface interrogation. Interrogation techniques attempt to illuminate curve and surface characteristics that are not easily discernible using conventional rendering. They usually exaggerate shape to make it easier to detect a curve's or surface's subtle aspects or flaws. Many surface interrogation methods have been proposed Moreton [1] surveyed various interrogation techniques used in curve and surface design and evaluation. Forrest [2] discussed a variety of techniques for increasing the information content and the understandability of renderings of curved surfaces. Klass [3] evaluated and faired curved surfaces using the lines of reflection, i.e. the images of parallel lines reflected on a smoothly curved surfaces. Dill [4] discussed the assessment of curved surfaces on the basis of pseudo coloring that represents mean curvature and Gaussian curvature. Hoscheck [5] described the use of polarity to expose inflections in curves, and areas of zero Gaussian curvature in surfaces. Bech et al.[6] compared analysis techniques, including shaded renderings, contours of intensity, curvature, lines of principal curvature, geodesic paths, and curvature pseudo coloring. Munchmeyer [7] presented a case study of surface analysis techniques relating to the display of contours of Gaussian curvature, mean curvature, maximum principal curvature, principal directions, asymptotic directions, and level contours. Higashi et al. [8] presented curve and surface analysis techniques that draw closely spaced radii of curvature along curves and planar sections of surfaces. Finally Pottmann [9] provided simple examples where lines of reflection fail to expose discontinuities of curvature. He described a new approach designed to maximize the apparent curvature discontinuity at patch to patch boundaries.

In this paper, two types of interrogation methods for the assessment of shape quality are described. One is the reflection mapping, which simulates the reflection test on the real part in the production line. The other is the visualization of the curvature behavior of a surface using

the focal surface.

Reflection mapping was developed to model specular inter-object reflection by Blinn and Newell [10] (see Reference [11] for more details). A center of projection, usually being the center of the objects to be rendered, is chosen and used as the center of a virtual sphere surrounding the objects. Then the environment is projected onto the surface of the virtual sphere. This virtual ball can then be treated as a 2D texture map, i.e. reflection map. At each point on an object to be displayed, the corresponding location in the reflection map is found by reflecting the view vector about normal vector of the object at the point. The reflection map's x and y axes represent longitude (from 0° to 360°) and latitude (from -90° to 90°), respectively, as shown in Figure 1. For the purpose of surface interrogation, we replace spherical environmental map with virtual box which has striped line patterns on its each face. Thus, one can evaluate the surface quality by comparing mapped images onto the surface with original images on the reflection map.

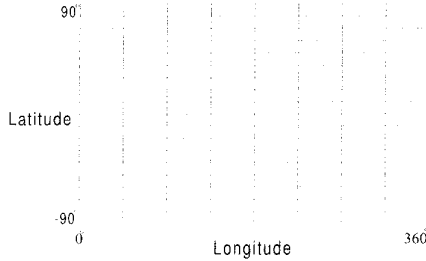


Figure 1. Reflection map coordinate systems.

Focal surfaces are equivalent to functional offset surfaces in the context of surface interrogation. A functional offset surface is a surface offset from a subject surface by an amount controlled by a function, typically, of the subject surface's geometry. We use mean, Gaussian and strain energy of curvature as offset function in this work. This curvature functions enable curvature properties and undesired regions to be visualized at the same time.

Since we implemented the reflection mapping and the focal surface for the surface approximated by triangulation facets, we will describe briefly the triangulation algorithm first. Reflection mapping is described in the third section and the focal surface in the fourth section. The fifth section will summarize the main results.

2. Triangulation of trimmed surfaces

A trimmed surface consists of base surface and boundary curves, i.e. trimming curves. Boundary, i.e.

trimming curves are defined as follows, Let base surface

$$S = S(u,v) = (x(u,v), y(u,v), z(u,v)) \quad (1)$$

be a regular parameterized surface whose domain is a rectangle defined by

$$D = \{(u,v) \mid u_1 < u < u_2 \text{ and } v_1 < v < v_2\} \quad (2)$$

Let $B = B(t)$ be a curve defined by

$$B(t) = (u(t), v(t)) \text{ for } a < t < b \quad (3)$$

taking its value in D so that it lies in the two dimensional parameter domain of the base surface.

A trimming curve $C(t)$ on the base surface $S(u,v)$ is the composition of two mappings, S and B defined as follows,

$$\begin{aligned} C(t) &\equiv S \circ B(t) \\ &\equiv S(B(t)) \\ &\equiv S(u(t), v(t)) \\ &\equiv S(x(u(t), v(t)), y(u(t), v(t)), z(u(t), v(t))) \\ &\quad (a \leq t \leq b) \end{aligned} \quad (4)$$

For the triangulation of a trimmed surface, i.e. generation of triangulation facets of a trimmed surface, we introduce the Delaunay triangulation algorithm using child loop concept. It consists of following procedures.

2.1. Boundary curve tessellation

In this step, boundary curves are approximated by a set of line segments, i.e. boundary line segments in the two dimensional parametric domain of the base surface (see Figure 2). Boundary line segments are directed such that the outer boundary has a counterclockwise direction, while the inner holes have clockwise directions. We will use this directional information to generate child loops for the efficient Delaunay triangulation. Every boundary segment is stored in a singly linked list as shown in Figure 3. If we have a hole loop, the linked list of the segment in the hole loop is attached to the linked list of the outer boundary. In Figure 3, start and end points have two dimensional (u,v) value of the parametric domain of the base surface

2.2. Node generation inside the trimmed region

To generate nodes inside the trimmed area of the given surface, which will be used as the vertices of facets in the triangulation step, we first construct iso-parametric lines corresponding to constant u values on the (u,v) domain of the base surface as shown in Figure 2. Then, intersections between these iso-parametric lines and the

boundary segments are calculated. In this process, all boundary segments are tested against the intersection. If a boundary segment is found to intersect, then the v value of the intersection point is inserted into v value table (as shown in Figure 4). Since there can be many intersections between an iso-parametric line and the boundary segments, these v values are stored in a linked list according to their magnitudes. Figure 4 shows a linked list for the iso-parametric lines with constant u values and intersection points between an iso parametric line and boundary segments. Note that nodes can exist from v value of odd order to that to even order as illustrated in Figure 5. We will call, these portions of each iso-parametric line live portions. For the live portions of each iso-parametric line, we generate nodes such that the adjacent nodes separated uniformly.

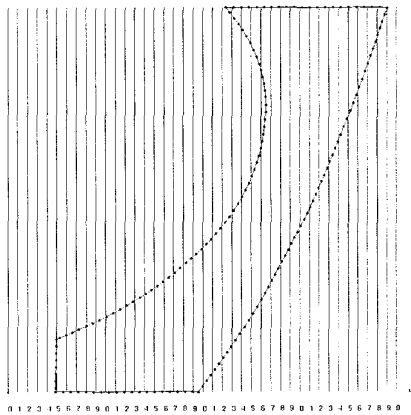


Figure 2. Boundary line segments

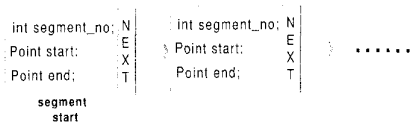


Figure 3. Data structure for boundary line segments

2.3. Child loop generation

We will use Delaunay triangulation algorithm to get facets from given nodes and boundary segments. Delaunay triangles are those triangles whose associated circumcircles contain no node points on their circumferences or in their interiors. Although Delaunay triangulation is a useful tool in generating facets, it is a time-consuming algorithm for a domain of many nodes like ours. This demerit comes from the fact that the algorithm searches for all nodes to find optimized Delaunay triangles. To overcome this problem, we

introduce the concept of child loop as shown in Figure 6. Child loop which is composed of nodes and boundary segments is a counterclockwise directional loop. Although there may be hole in trimming boundary, there is no hole in child loop. Delaunay triangulation can be performed efficiently by subdividing a trimmed surface into several child loops in the (u,v) parametric domain of the base surface(as shown in Figure 7).

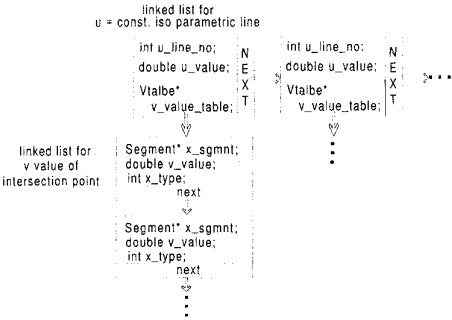


Figure 4. Data structure for constant u parametric lines

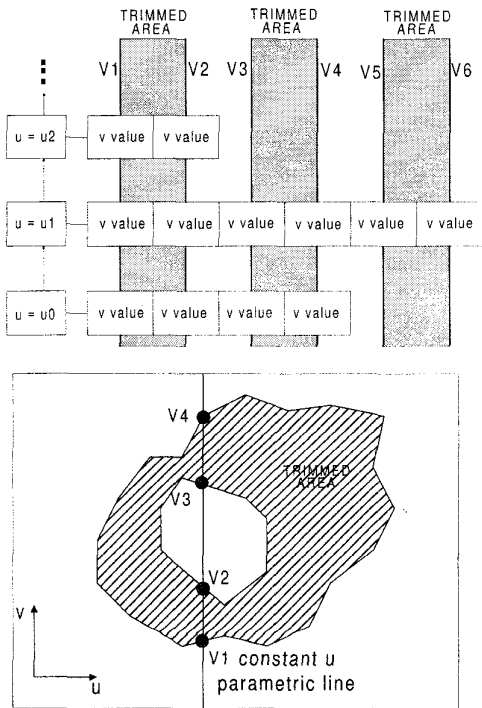


Figure 5. Trimmed area in the v value table

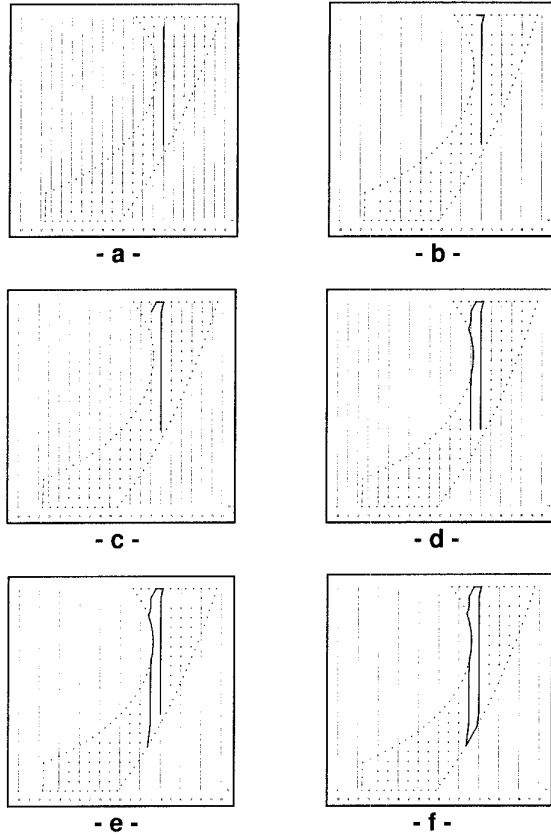


Fig. 6 Generation of a child loop.

2.4. Triangulation

Finally triangulation is performed for each child loop. Because child loop has no hole as mentioned above, triangulation can be simply performed through the following procedure for a given child loop.

- ① Take the first segment from the given child loop as a current segment.
- ② Find the third vertex satisfying Delaunay criterion by searching all the segments in the child loop except current segment.
Delaunay criterion can be stated as below.
 - For a given segment $\langle A, B \rangle$ the third vertex C should make $\cos \angle ABC$ minimum.
 - The triangle being formed should not cross any edge of the existing triangles in the linked list.
- ③ When third point is found, make a triangle and add it to the linked list.
- ④ Delete current segment from child loop.
- ⑤ Add edges of new triangle, if it does not exist in the child loop.
- ⑥ Triangulation is completed when child loop has no entity.

Figure 8 (a) shows the result of the triangulation in u, v domain and (b) shows the mapped image in real space.

3. Reflection Mapping

Our reflection mapping algorithm for surface interrogation consists of following five steps.

- 1st step: Construct reflection map consists of colored stripes on the rectangular box. The box should be large enough to include the surface being evaluated.
- 2nd step: Divide the surface to be evaluated into several facets, since we are using the facet model of the surface for the computational efficiency. Delaunay triangulation algorithm [12] mentioned in the previous section is applied in this step. Once the facet model is derived, following steps are performed for each facet.
- 3rd step: Determine the colors of three vertices of a given facet by finding the corresponding stripe of the reflection map.
- 4th step: Determine the color for the given facet from the result of previous step. In this step, the facet may be modified to result the smooth mapped boundary which corresponds to the stripe in the map.
- 5th step: Fill the facet with color obtained from 4th step.

We will explain each step in detail as below. The first step of the reflection mapping is to construct a reflection map. We used a virtual box enclosing the surface to be evaluated. The size of this box is easily determined from the range of the coordinates of the surface points. The patterns on the faces of the box are chosen considering the following aspects.

1. The comparison between the patterns on the reflection map and their mapped images on the subject surface should describe the shape quality of the surface well.
2. The calculus involved in the mapping should be simple and require simple calculation.

From the considerations above, the striped line pattern is chosen because it is easy to compare the straight line image on the map with the distorted mapped image on the subject surface and to compute intersections between line and line. Thus the resulting reflection map box has information about planar equations, the number of striped lines, colors of each striped line for all six faces. Figure 9. shows a reflection map box chosen in this work. The width of the stripe is determined such that the colored and the uncolored stripes have the same width as shown in Figure 9.

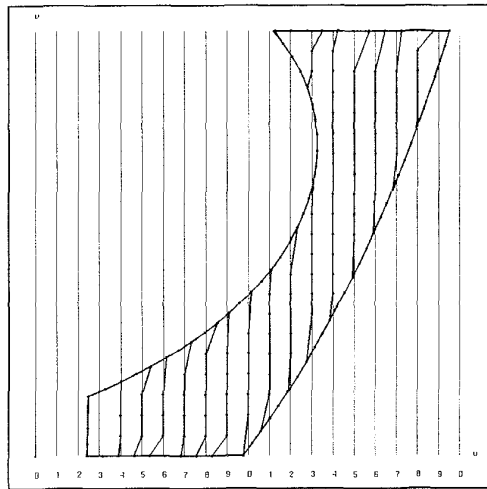
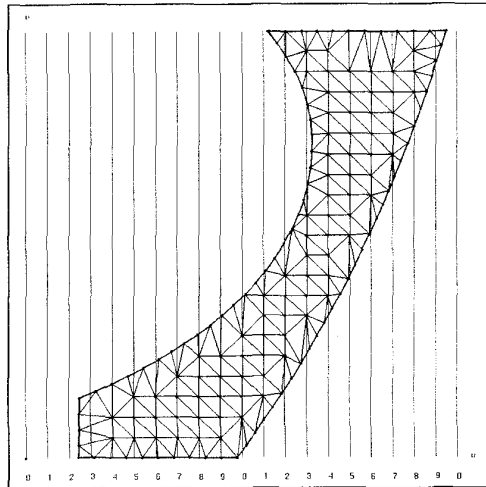
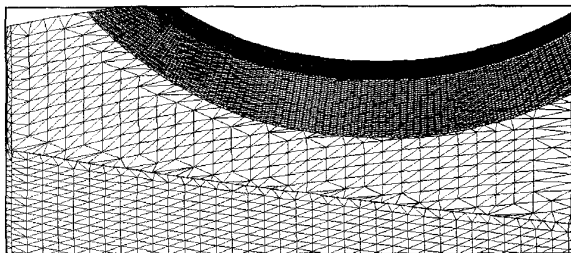


Fig. 7 Subdividing of a trimmed surface into several child loops.



a. Parametric domain.



b. Real space.

Figure 8. The result of triangulation .

Once a reflection map box is defined, mapping is performed. Since this process is carried out for each facet in our algorithm, the surface should be divided into

several facets. We used Delaunay triangulation algorithm introduced in the previous section. Since this triangulation is performed on the (u,v) parametric domain of the test surface, each facet has three two dimensional (u,v) points as their vertices as shown in Figure 10.

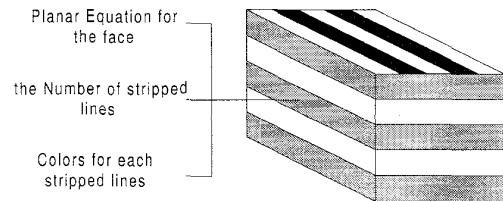


Fig. 9 Reflection map box.

POINT vertex1	N	POINT vertex1	N	
POINT vertex2	E	POINT vertex2	E	...
POINT vertex3	X	POINT vertex3	X	
Color color	T	Color color	T	

Figure 10. Linked list for facets.

For a given facet, reflection mapping begins with the determination of colors of its three vertices. The color of a vertex, i.e. the color of the corresponding point on the reflection map, is determined through the following steps.

- ① Find the position vector P of the given vertex as shown in Figure 11.
- ② Calculate view vector E from the vector equation $E = e - P$ where e is the position vector for viewpoint.
- ③ Calculate the normal vector N of the given surface at P
- ④ Find the relative reflection vector R satisfying the following two conditions.
First: relative reflection vector R must be on the same plane which N and E make.
Second: the angle between N and E must be equal to that of N and R .

These two conditions are equivalent to say that the color at point P felt by the viewpoint is the color of the image which will reflect at point P in the viewpoint direction assuming the perfect specular reflection.

- ⑤ Find relative reflection line L which passes through P and whose directional vector is R .
- ⑥ Calculate the intersection between L and reflection map box. This can be obtained from the planar equations of the map and the equation of L .
- ⑦ Determine the color of a given vertex to be the color of the stripe to which the intersection point obtained in ⑥ belongs.

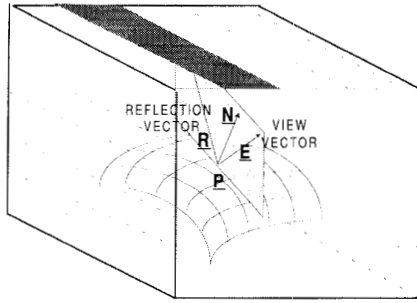


Figure 11. Reflection mapping.

Once the colors of all vertices of a facet are determined, the color of the facet is to be determined. Based upon the uniformity of the vertex colors, we can categorize the situation in three cases as shown in Figure 12.

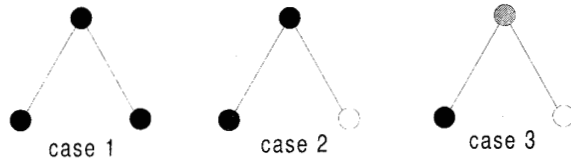


Fig. 12 Categorization based upon uniformity of vertex colors

Case 1: Three vertices of a facet have the same color. In this case the facet is assigned the same color as its vertices. This will give a practically correct result if the facet size is pretty small. For a small facet, we can assume that the corresponding region in the reflection map is a triangle and the triangle resides in the same stripe when all of its vertices are inside the stripe.

Case 2: If the color of one vertex is different from other two vertices, the facet should be divided into four facets f1, f2, f3 and f4 from which approximate boundary segments are to be derived as shown in Figure 13. This process can be done by deleting the facet from the linked list of facets and inserting f1, f2, f3 and f4 instead. In the figure, point b3 is simply the middle point of points v1 and v2. Point b1 can be obtained from the intersection between line $\overline{v'1v'3}$ and the boundary line L on the map. Here $v'1$ and $v'2$ are the mapped points of points v1 and v3 onto the reflection map respectively. Once the intersection is obtained on the reflection map, the corresponding point b1 of the facet is derived in the parametric domain by applying the scale factor $\overline{v'1b'1}:\overline{b'1v'3}$ to $\overline{v1b1}:\overline{b1v3}$ as shown in the following equations. b2 is also

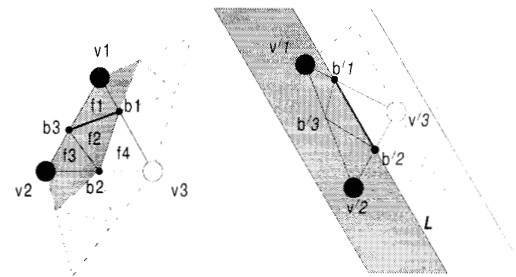
derived through the same way. This is of course an approximation which works for a small facet.

$$b1(u,v) = \frac{\overline{v'1 - b'1} \overline{v3(u,v)} + \overline{b'1 - v'3} \overline{v1(u,v)}}{|\overline{v'1 - v'3}|} \quad (5)$$

$$b2(u,v) = \frac{\overline{v'2 - b'2} \overline{v3(u,v)} + \overline{b'2 - v'3} \overline{v2(u,v)}}{|\overline{v'3 - v'2}|} \quad (6)$$

$$b3(u,v) = \frac{\overline{v1(u,v)} + \overline{v2(u,v)}}{2} \quad (7)$$

Then the colors of facets f1, f2 and f3 become that of the vertex v1. Similarly facet f4 has the same color as the vertex v3.



(a) Facets on the (u,v) domain of the surface

(b) Facets on the reflection map

Figure 13. Subdivision of a facet into four facets.

Case 3: If all the vertices have the different colors, the facet should be subdivided until all the subdivided facets can be classified to be either case 1 or case 2.

Once all facets have their own colors, they are filled with their colors as illustrated in Figure 14. Figure 14 shows the surfaces constituting fender of a car with reflection mapped. This model consists of 14 trimmed surfaces.

The result shown in Figure 14 may not look like a realistic shape. Thus we applied rendering effects to our mapping algorithm using the shading facilities of GL graphics libraries [13]. This can be done by simply assuming that the light for any point on the test surface is comes from the corresponding point on the reflection map. The color of the light is also the color of the corresponding stripe. The view point is the same as that we used for the reflection mapping. The resulting image is shown in Color Plate 1.

From the result of reflection mapping, we can interpret the global behavior of the curvature and the normal vector of the test surface. From Color Plate 1. we can

induce the fact that the magnitude of curvature is relatively small in the region where the widths of mapped stripes are wide (area D in Color Plate 1). The winding pattern of the mapped stripe (area B in Color Plate 1) also indicates that the normal vector of the subject surface varies irregularly. The discontinuities in area C may tell that the similar phenomena occurs in the behavior of the normal vector. Figure 15 shows these facts clearly. In Figure 15, one can infer that there are some problems in the shape quality from the distorted and discontinuous mapped striped line images inside the area A. The various colors of the stripes in the region A means that many different faces of the reflection map box are reflecting on that region. This means that the region has relatively large value of curvatures and wide range of normal vectors. The other marked area in Figure 15 shows similar problems as in A. The same conclusion can be derived from the focal surface analysis to be followed.

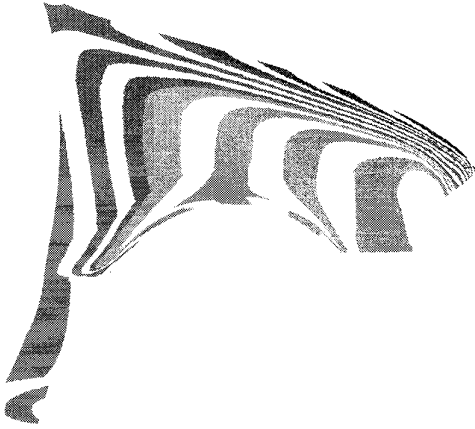


Figure 14. Example result of reflection mapping.

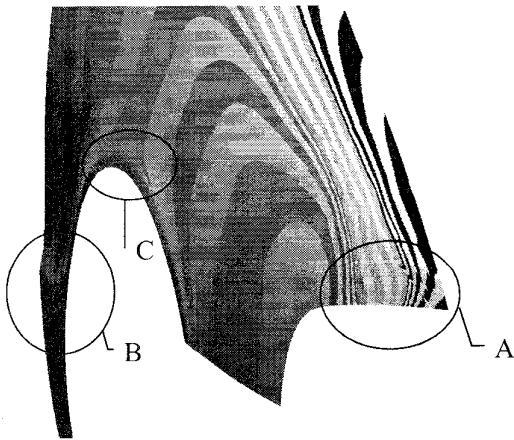


Fig. 15 Undesirable design area

4. Focal surfaces

The generalized focal surface concept was proposed by Hagen and Hahmann [14] and it is based on the following formula:

$$F(u, v) = X(u, v) + a \cdot f(\kappa_1, \kappa_2) \cdot N(u, v) \quad (8)$$

where, a is scale factor and f is a scalar function of the two principal curvatures $\kappa_1(u, v)$ and $\kappa_2(u, v)$. The scale factor a is necessary to distinguish the focal surface from the surface being tested, because curvatures have small values. The function f can be any real scalar valued function of principal curvatures and we used Gaussian, mean and strain energy of curvature as that function in this work.

As mentioned in the previous section, we assume that the test surface has been divided into several facets and the focal surface is generated for each facet. The following procedure is performed for each facet.

1. For each vertex of a given facet, find the corresponding focal point using the following equation

$$F_{focal_point}(x, y, z) = X_{vertex}(x, y, z) + a \cdot f(\kappa_1, \kappa_2) \cdot N_{vertex}(x, y, z) \quad (9)$$

2. Rendering both facet, one from the test surface and the other from the focal surface, with different rendering settings

Color Plate 2 illustrates the test surface and the focal Gaussian surface. Gaussian curvature characterizes the shape of a surface patch as follows. If $K > 0$ (elliptic points), then the surface patch has elliptic form, i.e., it is convex; If $K < 0$ (hyperbolic points), then the surface patch has saddle form; and if $K = 0$ (parabolic points), then the surface patch has cylindric form. Therefore, one may be interested in the change of sign in the Gaussian curvature, which is the property owned by the undesired inflection points of curves. We can expect that the Gaussian curvature changes its sign where the focal Gaussian surface and the test surface intersect. The marked area B in Color Plate 2 corresponds to these locations. The marked area A where oscillations occur in the focal Gaussian surface describes the fact that the similar situations occur in the behavior of the curvatures of the test surface.

Similarly, the mean curvature $f = \frac{1}{2}(\kappa_1 + \kappa_2)$ can be

visualized as in Figure 17 Mean curvature is a measure whose magnitude is of sole importance, and the sign of mean curvature is dependent on surface orientation. Mean

curvature is zero when a surface is ‘perfectly’ hyperbolic, i.e. when it has principal curvatures of equal magnitude but opposite sign. Minimal surfaces, surfaces of minimum area, have zero mean curvature. From the result in Figure 17, one can tell that there are some shape irregularities especially in the marked region A, B and C. As was inferred from the focal Gaussian surface, undulations occur in the region A of the focal mean surface. In the figure, the sudden jump of focal mean surface indicates the region with the relatively large curvature. This is consistent with the results of the reflection mapping.

To gain a new insight into the general curvature behavior, it is simply necessary to change the function f of the curvature. Strain energy of curvature $f = \kappa_1^2 + \kappa_2^2$ is a nonnegative measure that simply indicates the extent to which a surface is deviated from a plane. It does not provide any indication of surface type. The function $f = \kappa_1^2 + \kappa_2^2$ can also be used to detect flat points, where the principal curvature vanish identically ($\kappa_1 = \kappa_2 = 0$). Flat points or flat regions are usually undesirable. A convex surface with flat points appears to have dents, which is not aesthetically pleasant. A focal surface for the strain energy of curvature is illustrated in Figure 18. In the figure, we can see that there is no flat point. The function $f = \kappa_1^2 + \kappa_2^2$ can also be used to visualize the continuity of the surface. The order of continuity of the generalized focal surface is less than that of the test surface by 2. This means that a surface of class C^3 has a generalized focal surface of class C^1 . Thus a surface with a non-continuous focal surface for the strain energy of curvature can be maximally of class C^1 .

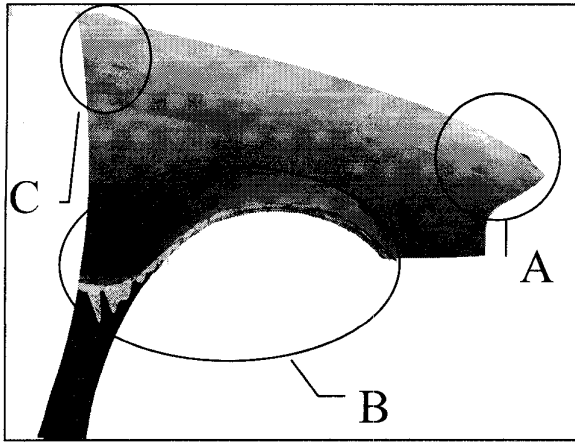


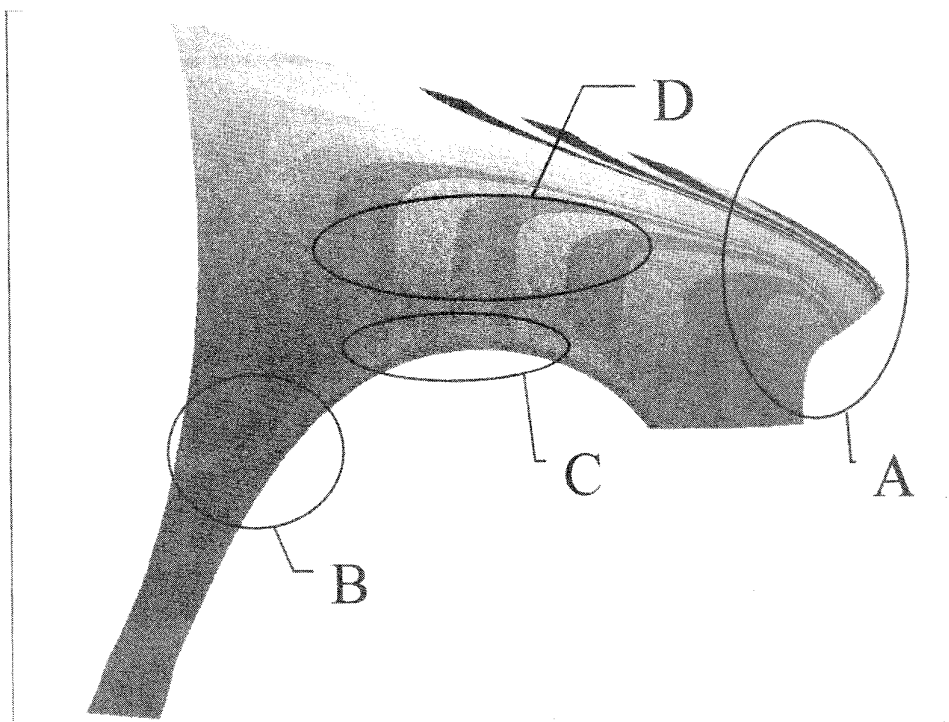
Fig. 18 Focal mean surface



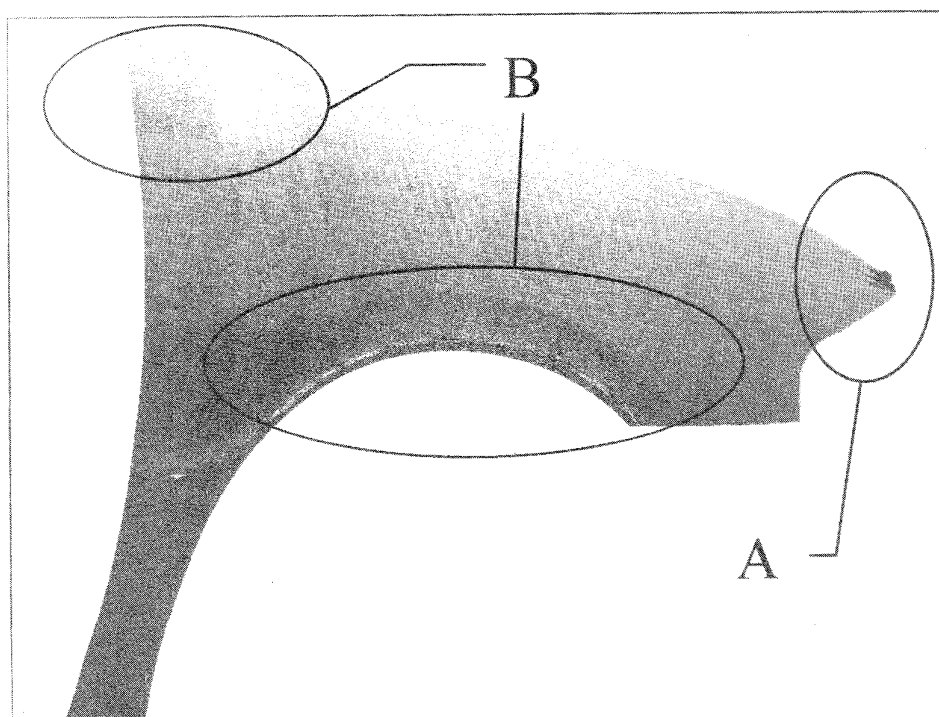
Fig. 18 Focal surface using strain energy of curvature

5. Conclusions

We described two methods for the surface interrogation. The reflection mapping algorithm using a simple reflection map could simulate the physical reflection phenomenon efficiently. With reflection mapping analysis, a global check for the shape quality is possible. One can evaluate a surface quality in terms of curvature and normal vector using this method. In addition to the reflection mapping, focal surfaces provide an excellent means of analysing and comparing the curvature characteristics of the surfaces. The various curvature functions enable the curvature properties and irregular regions to be visualized at the same time.



Color Plate 1. Reflection mapping with shading effect.



Color Plate 2. Focal Gaussian Surface.

For color plate see page 251

References

-
- [¹] Henry P Mreton 'Simplified curve and surface interrogation via mathematical packages and graphics libraries and hardware' *Comp. Aided Des.* Vol 27 (1995) pp 523-543
- [²] Forrest, A R 'On the rendering of surfaces' *Comput. Graph.* Vol13(Aug 1979)pp 253-259
- [³] Klass, R 'Correction of local surface irregularities using reflection lines' *Comput.-Aided Des.* Vol 12 (Mar 1980) pp 73-77
- [⁴] Dill, J C 'An application of color graphics to the display of surface curvature' *Compu.Graph.* Vol15 (Aug 1981) pp 153-161
- [⁵] Hoschek, J 'Detecting region with undesirable curvature' *Comp. Aided Geom. Des.* Vol 1 (1984) pp 183-192
- [⁶] Beck, J M, Farouki, R. T. and Hinds, J K 'Surface analysis methods' *Comput. Graph. & Applic.* Vol 6 (Dec 1986) pp18-36
- [⁷] Munchmeyer, F 'On surface imperfections' in the *Mathematics of surfaces II* Oxford University Press, USA (1987) pp 459-474
- [⁸] Higashi, M, Kaneko, K and Hosaka, M 'Generation of high quality curves and surfaces with smoothly varying curvature' *Proc. Eurographics'88 Conf.*(12-16 Sep 1988) pp 79-92
- [⁹] Pottmann, H 'Visualizing curvature discontinuities of free-form surfaces' *Proc. Eurographics '89 Conf.* (1989) pp529-536
- [¹⁰] Blinn, J.F., and M.E. Newell 'Texture and Reflection in Computer Generated Images,' *CACM*, 19(10), October pp542-547
- [¹¹] Foley, van Dam, Feiner, Hughes, *Computer Graphics* Addison-Wesley (1990)
- [¹²] SeungWook-Jung, 'Constrained Delaunay Triangulation' (1994)
- [¹³] *Graphics Library Programming Guide*
- [¹⁴] Hagen, H and Hahmann, S 'Generalized focal surfaces: a new method for surface interrogation' *Proc. Visualization '92 Conf.* Boston MA, USA (1992) pp70-76